Magnetic and transport properties of evaporated Fe/SiO multilayers

M. Anas, C. Bellouard, M. Vergnat

Magnetic and transport properties of evaporated Fe/SiO multilayers

M. Anas
Haluoleo University, Kampus Bumi Tridharma Kendari 93231, Indonesia

C. Bellouard and M. Vergnat
Laboratoire de Physique des Matériaux, (UMR CNRS No 7556), Université Henri Poincaré Nancy 1, Boîte Postale 239, 54506 Vandœuvre-lès-Nancy Cedex, France

(Received 3 March 2004; accepted 24 April 2004)

Fe/SiO discontinuous multilayers consisting of layers of Fe particles embedded in an insulating SiO matrix have been prepared by evaporation. Their structural, magnetic, and transport properties have been studied as a function of Fe and SiO thickness. For small iron thicknesses, magnetic measurements show a superparamagnetic behavior above a blocking temperature determined by field-cooled and zero-field-cooled magnetization curves. Negative magnetoresistance due to spin-dependent tunneling has been observed in both current-in-plane and current-perpendicular-to-the-plane geometries. For the smaller iron thickness (5 Å), a Coulomb blockade effect is observed at low temperature together with an increase of the magnetoresistance. © *2004 American Institute of Physics.* [DOI: 10.1063/1.1762998]

I. INTRODUCTION

Tunnel magnetoresistance (TMR) was experimentally observed by Julliere[1] in Fe/Ge/Co and Fe/Ge/Pb junctions. The large magnetoresistance (MR) response in low magnetic fields has stimulated considerable interest. However, fabricating pinhole-free insulating barriers remains a major problem. MR was also observed in codeposited granular metal/insulator (cermet) films[2] which consist of randomly distributed ferromagnetic particles in an insulating matrix. For applications, these films are easier to fabricate, are very robust due to the protective insulating oxide and are not as susceptible to electrical breakdown as tunnel junctions. Transition metals, mainly, Co and Fe, and their alloys have been used to get magnetic granules. The insulating matrices were: Al_2O_3,[3–6] SiO_2,[7–8] MgF_2,[9–10] Cr_2O_3,[11–12] PbO_x,[13–14] TaO_x[15] or MoO_x.[16] Very low MR ratio (<1% at 300 K) was found with TaO_x or MoO_x whereas a maximum effect close to 10% at room temperature has been observed with systems as Co and CoFe-Al_2O_3, Co-MgF_2, and Fe-PbO_x where a magnetic Fe_2O_3 compound is formed between the magnetic grains and the insulating matrix. However, the saturation fields (at least several kOe) are much too high for application purposes.

Discontinuous metal/insulator multilayers constitute another class of granular films consisting of well-separated planes of closely spaced ferromagnetic nanoparticles in an insulating matrix. They present the same advantages than cermet films, with much lower saturation fields. Moreover, the very anisotropic morphology of discontinuous multilayers offers new fundamental physical behaviors with respect to cermets films as their transport properties depend strongly on the measurement geometry: ''CIP'' with current in plane of the layers or ''CPP'' when the current is perpendicular to the layers. The CIP properties are usually close to those of the cermet[17] whereas specific voltage and temperature dependences of resistance and MR (with eventually an enhancement) have been observed in the CPP geometry due to the Coulomb blockade effect.[4,18–22] The tunneling of an electron into a neutral cluster is stopped when thermal energy and applied voltage are much smaller than the charging energy of a cluster. Because of their large response observed in granular alloys, Co/Al_2O_3,[19,23,24] $CoFe/Al_2O_3$,[17,25,26] Co/SiO_2[21,27] have been extensively studied and new systems as $CoFe/HfO_2$,[20] Co/ZrO_2,[28] or Fe/ZrO_2,[29] have been investigated. The discontinuous multilayers were always deposited by sputtering with eventually an annealing process. Their thicknesses were typically about 10–20 Å for the metal and 30–40 Å for the oxide.

We have recently performed a study of the structural and transport properties in coevaporated Fe_xSiO_{1-x} granular films[30] as a function of the Fe volume fraction x. It has been shown that a superparamagnetic behavior is obtained for $0.13 \leqslant x \leqslant 0.27$ together with a MR tunnel effect for $0.2 \leqslant x \leqslant 0.27$. The amplitude of the MR effect is rather low, of the order of 2% at 100 K. An annealing at a moderate temperature (300 °C) does not modify significantly this effect, it decreases drastically for a higher annealing temperature.[31] These results have been interpreted by the presence of an FeSi alloy at the interface between granules and the matrix which damages the polarization of electrons. In the present study, in order to limit the chemical mixing at the interface, discontinuous Fe/SiO multilayers are investigated. Their structural characterization have been performed using x-ray reflectivity and transmission electron microscopy. Magnetic characterization has been done as a function of temperature and of applied field. Their magnetotransport properties have been checked in the CIP and CPP geometries.

II. EXPERIMENTAL DETAILS

Fe/SiO multilayers were deposited by evaporation of Fe and SiO from an electron beam and a thermal cell, respectively. The base pressure of the chamber was 10^{-8} Torr. The

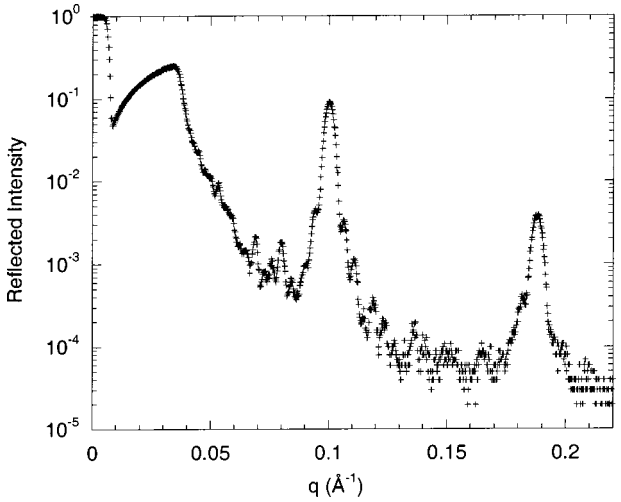

FIG. 1. Low angle x-ray reflectivity vs the scattering vector **q** of a $[SiO(70\,Å)/Fe(5\,Å)]_{20}$ multilayer.

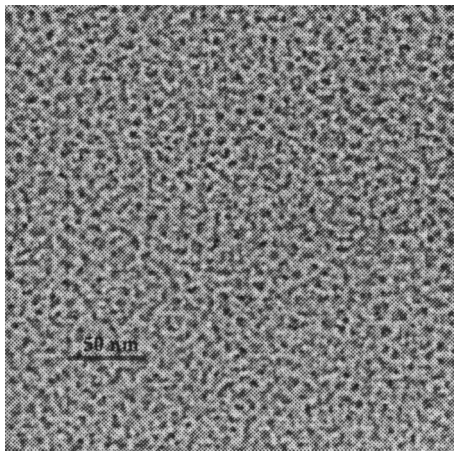

FIG. 2. Transmission electron microscopy micrograph of a SiO(90 Å)/Fe(8 Å)/SiO(90 Å) trilayer.

thickness of the layers have been measured using quartz oscillating sensors. A specific calibration using x-ray reflectivity has been made with a single thick SiO layer. The density of the deposited SiO layer is much lower than the density of the bulk material by roughly a factor 1.5. The deposition rate was 0.2 Å/s for Fe and 1 Å/s for SiO. The substrates were maintained at 100 °C. The iron layer thickness t_{Fe} evaluated from the mass measured by the quartz oscillator and the bulk density has been varied from 5 to 15 Å. The SiO layer thickness t_{SiO} evaluated from the specific calibration was varied from 70 to 110 Å. The number of bilayers was between 15 and 25.

For magnetic and electrical measurements, the films were deposited onto silicon and float glass substrates, respectively. The magnetic properties were determined with a semiconducting quantum interference device magnetometer. Field-cooled (FC) and zero-field-cooled (ZFC) magnetization measurements have been performed as a function of increasing temperature for an applied field of 20 Oe.

The multilayers for transport measurements were deposited with shadow masks designed for measurements with the current perpendicular to the plane or in the plane of the film. In the CPP geometry, the junction area is $(0.2\ \text{mm})^2$. For the CIP measurement, the current flows along a $5\times0.1\ \text{mm}^2$ stripe. Magnetoresistance was measured in a superconducting coil equipped cryostat with a maximum field of 70 kOe. The magnetoresistance is defined by $\text{MR}(H)=[R(H=0)-R(H)]/R(H=0)$.

III. EXPERIMENTAL RESULTS

A. Structural Characterization

The structure of the multilayers was studied by TEM. Diffraction patterns show two large and diffuse rings when the thickness t_{Fe} of the Fe layers was less or equal to 10 Å. The layers contained well-crystallized iron for $t_{Fe}=15$ Å. However, the composition modulation was always well observed even for very small iron thickness, as shown by the x-ray reflectivity spectrum (Fig. 1) of a $[Fe(5\,Å)/SiO(70\,Å)]_{20}$ multilayer where two superlattice Bragg peaks are observed. It corresponds to a periodicity of 68 Å close to the sum of the expected thicknesses. In-plane TEM micrograph for a [SiO(90 Å)/Fe(8 Å)/SiO(90 Å)] trilayer is shown in Fig. 2. The iron clusters forms chains which seem to be composed of several touching circular particles. This picture is similar to that obtained by Maurice and collaborators[23] for a $Al_2O_3/Co/Al_2O_3$ sample with a 15 Å Co thickness whereas they observed isolated iron grains for 7 Å Co thickness. We note that even for a 5 Å thick Fe layer, isolated grains are not observed, there are already clusters of several particles. This means that Fe spreads on the SiO surface unlike Co on Al_2O_3 which forms grains.

B. Magnetic properties

For $t_{Fe}=5$ Å and $70\,Å\leqslant t_{SiO}\leqslant 110\,Å$, the FC and ZFC curves are characteristic of granular systems [Fig. 3(a)]. They exhibit a 1/T type slope at high temperatures and a narrow peak of the ZFC curve for the so-called blocking temperature T_B which is equal to 15 K. For $t_{Fe}=8$ Å and $t_{SiO}=90$ Å, the bifurcation temperature (temperature above which the curves FC and ZFC superimpose) is now 60 K. Moreover, the low-temperature spontaneous magnetization of the ZFC curve is important. This proves the existence of a ferromagnetic coupling between the clusters. The increase of magnetization with decreasing temperature above T_B is indeed steeper than a 1/T slope for both multilayers [Figs. 3(a) and 3(b)]. As a consequence, the temperature dependence of the low field magnetization cannot be only attributed to superparamagnetism but also includes a temperature dependence of the moment per particle. This could be due to a disordered alloy with a much lower Curie temperature than bcc iron. For $t_{Fe}=10$ Å and $t_{SiO}=90$ Å, the ZFC and FC curves do not show a 1/T behavior [Fig. 3(c)]. They are similar to those of a ferromagnetic material with a Curie temperature comprised between 400 and 500 K. This is the signature of the onset of magnetic percolation which appears for very thin layers (10 Å) in comparison with other systems. For instance, with the Co/SiO_2 system, Dieny *et al.*[21] still observe a blocking temperature of 220 K for a 15 Å/Co thick

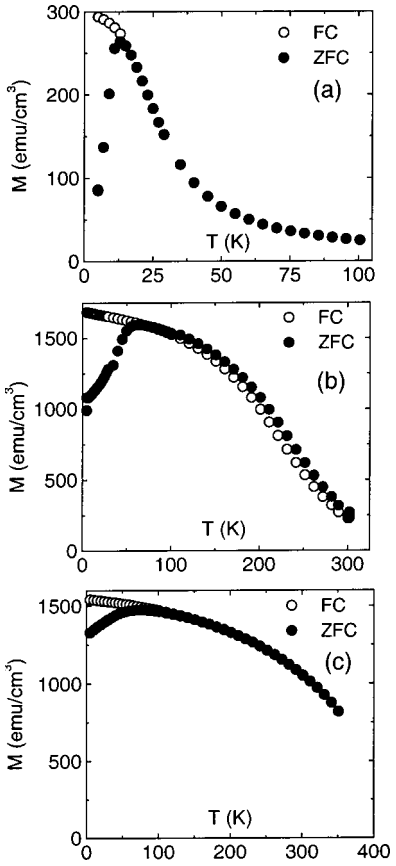

FIG. 3. Low field ($H=20$ Oe) magnetization measured as a function of temperature after field cooling (FC) or zero-field cooling (ZFC) for $[\mathrm{Fe}(t_{\mathrm{Fe}}\,\text{Å})/\mathrm{SiO}(90\,\text{Å})]_{15}$ multilayers with (a) $t_{\mathrm{Fe}}=5$ Å, (b) $t_{\mathrm{Fe}}=8$ Å, (c) $t_{\mathrm{Fe}}=10$ Å.

layer. This behavior of the Fe/SiO layers has to be directly related to the good wetting of Fe on SiO which was observed by TEM.

Figure 4 shows the evolution of the magnetization versus field for the $[\mathrm{Fe}(5\,\text{Å})/\mathrm{SiO}(70\,\text{Å})]_{15}$ multilayer at different temperatures. To get an order of magnitude of the size of the granules, the magnetization has been fitted by a sum of two Langevin functions at 60 K, above the blocking temperature. The use of two functions just allows to take into account the size distribution, but does not mean that there is two distinct

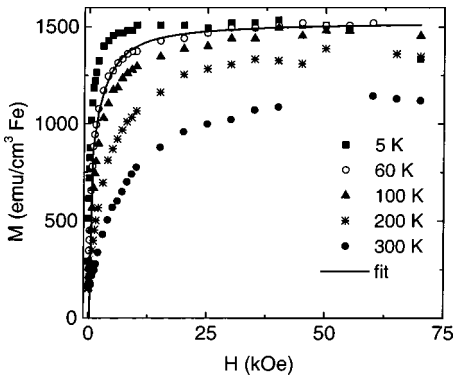

FIG. 4. Magnetization vs applied field for the $[\mathrm{Fe}(5\,\text{Å})/\mathrm{SiO}(70\,\text{Å})]_{25}$ multilayer at different temperatures. The straight line corresponds to a fit by a sum of two Langevin functions at $T=60$ K.

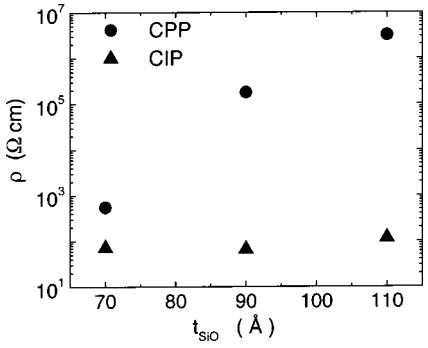

FIG. 5. CIP and CPP resistivity measured at 300 K of $[\mathrm{Fe}(5\,\text{Å})/\mathrm{SiO}(t_{\mathrm{SiO}})]_{15}$ multilayers as a function of t_{SiO}.

sizes of particles, only the mean size has a physical meaning. A mean moment per particle of $1400\mu_{\mathrm{B}}$ is obtained for $t_{\mathrm{Fe}}=5$ Å. The same treatment performed at 300 K for $t_{\mathrm{Fe}}=8$ Å provides a moment per particle of $9000\mu_{\mathrm{B}}$. As it will be shown below, the in plane metallic percolation arises slightly above $t_{\mathrm{Fe}}=10$ Å. As a matter of fact, it seems reasonable to assume that the granules are ellipsoides with a height of the order of 15 Å. With a moment per Fe atom of $2.2\mu_{\mathrm{B}}$, the lateral size of the Fe grains is then 32 and 90 Å for $t_{\mathrm{Fe}}=5$ and 8 Å, respectively. If we pursue the comparison between SiO/Fe 8 Å/SiO and $\mathrm{Al_2O_3}/\mathrm{Co}\,15\,\text{Å}/\mathrm{Al_2O_3}$, for which the in-plane shape of the granules are similar, we remark that our estimated size coincides with the lateral size observed for the 15 Å thick Co layer. Nevertheless, in the latter case, the percolation threshold is slightly above 20 Å and the height of the granules is evaluated to 28 Å from high resolution TEM.[23]

We note that the magnetization at 5 K is higher than that measured with coevaporated alloys exhibiting the same blocking temperature.[30] The magnetic state of the grains has then been improved by the alternate deposition of Fe and SiO. Nevertheless, the magnetization is slightly reduced with respect to the magnetization of bulk bcc iron. Moreover, the saturation magnetization clearly decreases with increasing temperature. As was already mentionned, some iron, probably located at the particle surface, remains disordered or poorly magnetized. Previous experiments performed with small angle neutron scattering have shown that Fe has no reduction of interface magnetization in Fe-SiO multilayers grown on a substrate cooled at liquid nitrogen temperature.[32] As a consequence, the damage of the interface in our experiment should be attributed to the higher substrate temperature (100 °C).

C. Transport properties

The resistivity ρ of multilayers with different Fe or SiO thicknesses was measured between 77 and 300 K. For t_{Fe} less than 10 Å, the samples present a semiconductor behavior with an increase of the resistivity when the temperature decreases. For $t_{\mathrm{Fe}}=10$ Å, the CIP resistivity is almost constant between 300 and 77 K, this thickness is then close to the metallic percolation.

The evolution of the resistivities measured at 300 K in the CIP and CPP geometries are presented in Figs. 5 and 6 as

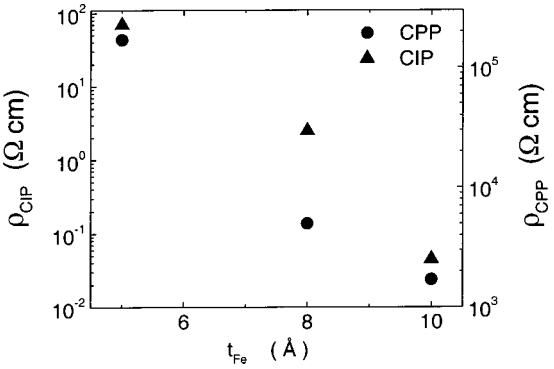

FIG. 6. CIP and CPP resistivity measured at 300 K of $[\mathrm{Fe}(t_{\mathrm{Fe}})/\mathrm{SiO}(90\ \text{Å})]_{15}$ multilayers as a function of t_{Fe}.

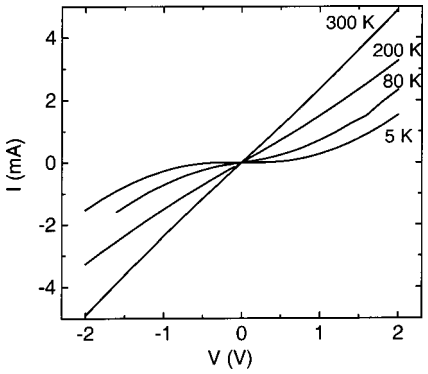

FIG. 8. $I(V)$ characteristics of a $[\mathrm{Fe}(5\ \text{Å})/\mathrm{SiO}(70\ \text{Å})]_{15}$ multilayer measured at different temperatures between 5 and 300 K in the CPP geometry.

a function of the SiO and Fe thickness, respectively. A steep increase of the CPP resistivity is observed as the SiO thickness is increased whereas the CIP resistivity is almost constant (Fig. 5). In the CPP geometry, the increase of t_{SiO} induces an increase of the barrier between grains, whereas in the CIP geometry, the current flows through the Fe layers without crossing the insulator layers. Both CIP and CPP resistivities strongly decreases with increasing Fe thickness (Fig. 6). The increase of the grain size with t_{Fe} induces an increase of the tunneling probability in both geometry. Moreover, in the CIP geometry, the decrease of the resistivity can also be attributed to the spreading of Fe in the plane which reduces the distance between the grains.

We remark that the CIP resistivity is always much lower than the CPP one. This is readily due to the strong anisotropy of the multilayers. Due to the specific growth of Fe on SiO, the distance between Fe grains in the plane is much lower than the distance between Fe planes. The CIP and CPP resistivities can then be tuned independently over orders of magnitude by varying the nominal thicknesses of the metallic and insulating layers.

Figure 7 shows the temperature dependence of the CIP and CPP resistivities of a $[\mathrm{Fe}(5\ \text{Å})/\mathrm{SiO}(70\ \text{Å})]_{15}$ multilayer. The behavior of the CIP resistance plotted in the inset is similar to that of a cermet: $\ln \rho_{\mathrm{CIP}}$ is linear as a function of $T^{-1/2}$ in agreement with the usual law for thermally activated tunneling: $\rho = \rho_0 \exp(2\sqrt{c_{\mathrm{CIP}}/kT})$ with a constant ρ_0 and c the activation energy. The fit provides $c_{\mathrm{CIP}} = 0.076$ eV; this value is close to the result obtained for the $\mathrm{Fe}_{0.27}(\mathrm{SiO})_{0.73}$ alloy ($c = 0.05$ eV).[30] On the contrary, as shown in the inset of Fig. 7, the CPP resistivity does not follow this law. According to the treatment proposed by Fettar *et al.*,[22] the temperature dependence of ρ_{CPP} has been fitted by

$$\frac{1}{\rho_{\mathrm{CPP}}} = \frac{1}{\rho_1}\exp\left[-2\left(\frac{c_{\mathrm{CPP}}}{kT}\right)^{0.5}\right] + \frac{1}{\rho_2}.$$

This expression assumes that there is an additional conduction path to the tunneling with a constant conductivity as already proposed.[33] It can be attributed to magnetic impurities.[22] From the fit plotted in Fig. 7, we deduce $c_{\mathrm{CPP}} = 0.112$ eV. This activation energy is function of the grain charging energy E_c, the separation between the grains s, the effective barrier ϕ, and the electron mass m: $c_{\mathrm{CPP}} = \sqrt{(m\phi/2\pi^2\hbar^2)}sE_c$. The x-ray reflectivity allows to evaluate the order of magnitude of $s = 60$ Å, the energy gap in SiO has been measured by optical experiments:[34] $\phi = 2.5$ eV, we then found $E_c = 90$ meV or a grain capacity of $C = e^2/2E_c = 9.10^{-19}$ F. Within the assumption of spherical particles, the diameter of the particles is given by $d = C/2\pi\epsilon_0\epsilon_r$. With the relative permittivity of SiO $\epsilon_r = 4$, we obtain $d = 40$ Å. This very crude model does not take into account the true shape of the particles, it provides nevertheless a right order of magnitude compared to the lateral size (32 Å) evaluated from magnetization measurement.

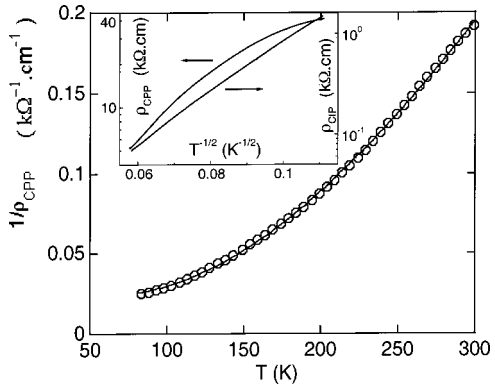

FIG. 7. Inverse of the CPP resistivity $1/\rho_{\mathrm{CPP}}$ of a $[\mathrm{Fe}(5\ \text{Å})/\mathrm{SiO}(70\ \text{Å})]_{15}$ multilayer as a function of temperature. The straight line corresponds to a fit by the expression: $1/\rho_{\mathrm{CPP}} = 1/\rho_1 \exp[-2(c_{\mathrm{CPP}}/kT)^{0.5}] + 1/\rho_2$. In the inset, the CIP and CPP resistivities, ρ_{CIP} and ρ_{CPP}, are plotted as a function of $T^{-1/2}$.

Figure 8 shows the CPP $I(V)$ curves of the same multilayer at different temperatures. At room temperature, the $I(V)$ curve is linear. When the temperature is decreased, a deviation from linearity appears clearly below 200 K in the range ± 2 V. When 1 V is applied to the sample with 15 SiO layers, only 70 mV is indeed applied on a junction. This voltage corresponds only to 2% of the energy gap of SiO, estimated to be about 2.5 eV.[34] As a matter of fact, the curvature of $I(V)$ is not due to the tunnel effect. Moreover, in that case, the $I(V)$ curve should be independent of temperature. Such behavior of $I(V)$ curves has already been observed in discontinuous multilayers and has been attributed to the Coulomb blockade effect.[4,18–22] The value of the Coulomb gap is given by the departure from zero of the $I(V)$

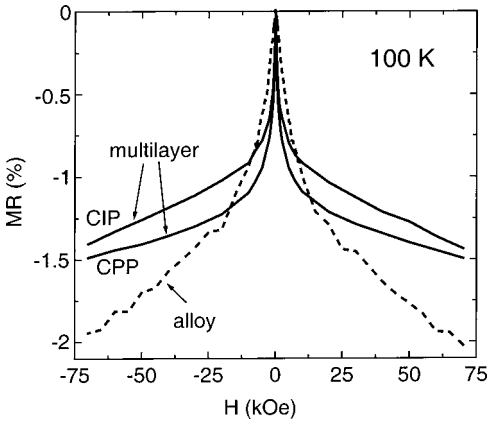

FIG. 9. CIP and CPP magnetoresistances as a function of applied field at 100 K for a $[\mathrm{Fe}(8\ \text{Å})/\mathrm{SiO}(90\ \text{Å})]_{15}$ multilayer and CIP magnetoresistance of a $Fe_{0.4}SiO_{0.6}$ alloy (at. %).

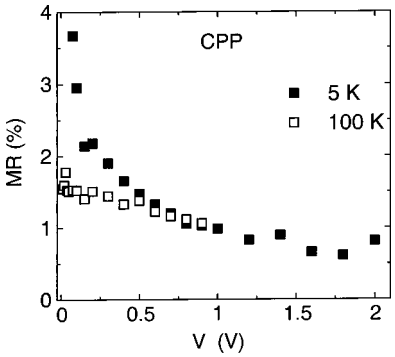

FIG. 10. CPP magnetoresistance measured as a function of applied voltage at 5 and 100 K for a $[\mathrm{Fe}(5\ \text{Å})/\mathrm{SiO}(70\ \text{Å})]_{15}$ multilayer.

curve. It is difficult to locate it in Fig. 8: this departure of $I(V)$ is not clear because of the particle size and shape distribution observed in TEM. If we consider that the gap begins at 0.8 V, it corresponds to a charge energy per particle of 800/15=50 meV. This value should correspond to the larger particles of the distribution. It seems reasonable compared to the mean value 90 meV deduced from the temperature dependence of the resistivity.

For the $[\mathrm{Fe}\,8\ \text{Å}/90\ \text{Å}]_{15}$ multilayer, the CPP $I(V)$ curves measured between ± 1 V are linear until 20 K, a deviation from linearity is only observed at 10 K and it appears clearly at 5 K. This behavior is due to the increase of the size of the particles with the Fe thickness, the charge energy is much then smaller, the Coulomb blockade cannot be observed in the same temperature range as for the previous sample.

D. Magnetoresistance

The magnetoresistance $\mathrm{MR}=[\rho(H)-\rho(0)]/\rho(0)$ was measured between 100 and 300 K for the $[\mathrm{Fe}(8\ \text{Å})/\mathrm{SiO}(90\ \text{Å})]_{15}$ multilayer. The MR values are represented in Fig. 9 for both CIP and CPP geometries with an applied voltage of 0.5 V. As in cermet films and tunnel junctions, the resistance is maximum when the degree of misalignment among the magnetizations of the particles is maximum. It decreases as the field is increased up to saturation. At low fields, there is a sharp response and, at high fields, the MR values are equal to 1.5% in both CIP and CPP geometries in the range 100–300 K. The $\mathrm{MR}_{\mathrm{CIP}}$ and $\mathrm{MR}_{\mathrm{CPP}}$ values observed with the $[\mathrm{Fe}(5\ \text{Å})/\mathrm{SiO}(70\ \text{Å})]_{15}$ multilayer are in the same order of magnitude: they are equal to 2.5 and 1.5%, respectively, at 100 K and they decrease to 0.9 and 0.3% at 300 K. For comparison the MR response of an alloy with a close atomic composition $Fe_{0.4}(SiO)_{0.6}$ has been plotted in Fig. 9. As was already observed with the $CoFe/HfO_2$ (Ref. 20) and Co/SiO_2 (Ref. 21) systems, the MR response at low field is better with the discontinuous multilayer. Nevertheless, the MR effect is low with both types of morphology. Its order of magnitude thus seems to be quite independent of the granules size and shape. It appears to be an intrinsic limit of the system. A systematic study devoted to coevaporated alloys performed with several techniques (magnetization, infrared spectroscopy, electron diffraction) has shown the presence of amorphous magnetic FeSi granules.[31] From the magnetization measurements presented above, the coexistence of an FeSi alloy with bcc iron in the multilayers cannot be ruled out.

The magnetoresistance measured for $H=70$ kOe as a function of applied voltage V in the CPP geometry is plotted in Fig. 10 for the $[\mathrm{Fe}(5\ \text{Å})/\mathrm{SiO}(70\ \text{Å})]_{15}$ multilayer. At 100 K, it increases weakly with decreasing voltage. At 5 K, the measurements are superimposed to the 100 K curve for $0.5\ \mathrm{V}<V<1\ \mathrm{V}$, below 0.5 V, a steep increase of the MR effect is observed which reaches 3.7% at 0.1 V. In the CIP geometry, the magnetoresistance exhibits a weak decrease with increasing voltage in the range $0<V<2$ V, similarly to the variation observed at 100 K in the CPP geometry. For the $[\mathrm{Fe}(8\ \text{Å}/\mathrm{SiO}(90\ \text{Å})]_{15}$ multilayer, the MR is flat as a function of the voltage for both geometries. As a matter of fact, we observe an enhancement of the MR in the voltage and temperature ranges of the Coulomb blockade regime. Such a behavior has already been observed in granular materials.[3,4,22,35] It has been attributed to a cotunneling effect: in the Coulomb blockade regime, when direct tunneling is ruled out, the transport of carrier from a charged large granule to a large neutral one is only possible via successive tunneling of single electron between small granules. As cotunneling is more sensitive to magnetic disorder than direct tunneling, the magnetoresistance is enhanced in the Coulomb blockade regime.[36,37]

IV. CONCLUSION

In conclusion, magnetoresistance at room temperature was observed in discontinuous Fe/SiO multilayers prepared by evaporation onto substrates maintained at 100 °C. Annealing was not necessary to obtain this phenomenon. Multilayers with iron thicknesses equal to 5 and 8 Å present a superparamagnetic behavior at room temperature. The occurrence of metallic percolation is close to 10 Å. The spin-dependent tunneling magnetoresistance is of the order of 1%–2% at 100 K and for 70 kOe, whatever the current direction (parallel or perpendicular to the layer) and the Fe thickness (5 or 8 Å). This effect is close to the result obtained with the coevaporated alloys. Its low amplitude appears as an intrinsic limit of

the system attributed to the presence of disordered FeSi alloy. Nevertheless, for $t_{Fe}=5$ Å, a Coulomb blockade effect is observed at low temperature with an enhancement of the MR.

[1] X. Julliere, Phys. Lett. **54A**, 225 (1975).
[2] Y. Goldstein and J. I. Gittleman, Solid State Commun. **9**, 1197 (1971).
[3] T. Zhu and Y. J. Wang, Phys. Rev. B **60**, 11918 (1999).
[4] S. Mitani, S. Takanashi, K. Takanashi, K. Yakushiji, S. Maekawa, and H. Fujimori, Phys. Rev. Lett. **81**, 2799 (1998).
[5] M. A. S. Boff, J. Geshev, J. E. Schmidt, W. H. Flores, A. B. Antunes, M. A. Gusmao, and S. R. Teixeira, J. Appl. Phys. **91**, 9909 (2002).
[6] A. Ya. Vovk, J.-Q. Wang, W. Zhou, J. He, A. M. Pogoriliy, O. V. Shypil, A. F. Kravets, and H. R. Khan, J. Appl. Phys. **91**, 10017 (2002).
[7] Q. Y. Xu, H. Chen, H. Sang, X. B. Yin, G. Ni, J. Lu, M. Wang, and Y. W. Du, J. Magn. Magn. Mater. **204**, 73 (1999).
[8] S. Honda and Y. Yamamoto, J. Appl. Phys. **93**, 7936 (2003).
[9] B. Hackenbroich, H. Zare-Kolsaraki, and H. Micklitz, Appl. Phys. Lett. **81**, 514 (2002).
[10] J. H. Chi, S. H. Ge, C. M. Liu, H. P. Kunkel, X. Z. Zhou, and G. Williams, J. Appl. Phys. **93**, 6188 (2003).
[11] S. Ge, Y. Liu, L. Xi, and C. Li, Phys. Status Solidi A **177**, R3 (2000).
[12] Y. Liu, L. Xi, C. Liu, and S. Ge, J. Magn. Magn. Mater. **226–230**, 685 (2001).
[13] Y.-H. Huang, J.-H. Hsu, J. W. Chen, and C.-R. Chang, Appl. Phys. Lett. **72**, 2171 (1998).
[14] J.-H. Hsu and Y.-H. Huang, J. Magn. Magn. Mater. **203**, 94 (1999).
[15] L. Kraus, O. Chayka, J. Tous, F. Fendrych, K. R. Pirota, M. Sicha, and L. Jastrabik, J. Magn. Magn. Mater. **226–230**, 669 (2001).
[16] D. Ishii, M. Koyano, S. Katayama, K. Higashimine, and N. Ohtsuka, J. Magn. Magn. Mater. **238**, 173 (2002).
[17] G. N. Kakazei, Y. G. Pogorelov, A. M. L. Lopes, J. B. Sousa, S. Cardoso, P. P. Freitas, M. M. Pereira de Azevedo, and E. Snoeck, J. Appl. Phys. **90**, 4044 (2001).
[18] S. Mitani, K. Takanashi, K. Yakushiji, J. Chiba, and H. Fujimori, Mater. Sci. Eng., B **84**, 120 (2001).
[19] L. F. Schelp, A. Fert, F. Fettar, P. Holody, S. F. Lee, J. L. Maurice, F. Petroff, and A. Vaurès, Phys. Rev. B **56**, R5747 (1997).
[20] S. Sankar, B. Dieny, and A. E. Berkowitz, J. Appl. Phys. **81**, 5512 (1997).
[21] B. Dieny, S. Sankar, M. R. McCartney, D. J. Smith, P. Bayle-Guillemaud, and A. E. Berkowitz, J. Magn. Magn. Mater. **185**, 283 (1998).
[22] F. Fettar, S.-F. Lee, F. Petroff, A. Vaures, P. Holody, L. F. Schelp, and A. Fert, Phys. Rev. B **65**, 174415 (2002).
[23] J. L. Maurice, J. Briatico, J. Carrey, F. Petroff, L. F. Schelp, and A. Vaurès, Philos. Mag. A **79**, 2921 (1999).
[24] D. Babonneau, F. Petroff, J.-L. Maurice, F. Fettar, A. Vaurès, and A. Naudon, Appl. Phys. Lett. **76**, 2892 (2000).
[25] W. Kleemann, O. Petracic, Ch. Binek, G. N. Kakazei, Y. G. Pogorelov, J. B. Sousa, S. Cardoso, and P. P. Freitas, Phys. Rev. B **63**, 134423 (2001).
[26] A. Dinia, G. Schmerber, C. Ulhaq, and T. El. Bahraoui, Mater. Sci. Eng., B **97**, 231 (2003).
[27] S. Sankar, A. E. Berkowitz, and D. J. Smith, Appl. Phys. Lett. **73**, 535 (1998).
[28] F. Ernult, L. Giacomoni, A. Marty, B. Dieny, A. Vedyayev, and N. Ryzhanova, Eur. Phys. J. B **25**, 177 (2002).
[29] P. Auric, J. S. Micha, O. Proux, L. Giacomoni, and J. R. Regnard, J. Magn. Magn. Mater. **217**, 175 (2000).
[30] M. Anas, C. Bellouard, and M. Vergnat, J. Appl. Phys. **88**, 6075 (2000).
[31] M. Anas, C. Bellouard, and M. Vergnat, J. Magn. Magn. Mater. (submitted)
[32] M. Sato, K. Abe, Y. Endoh, and J. Hayter, J. Phys. C **13**, 3563 (1980).
[33] S. Honda, T. Okada, and M. Nawate, J. Magn. Magn. Mater. **165**, 153 (1997).
[34] H. Rinnert, M. Vergnat, and G. Marchal, Mater. Sci. Eng., B **B69–70**, 484 (2000).
[35] H. Brückl, G. Reiss, H. Vinzelberg, M. Bertram, I. Mönch, and J. Schumann, Phys. Rev. B **58**, R8893 (1998).
[36] S. Takahashi and S. Maekawa, Phys. Rev. Lett. **80**, 1758 (1998).
[37] F. Guinea, Phys. Rev. B **58**, 9212 (1998).